*Article*

# Gasification Characteristics and Kinetics of Lipid-Extracted *Nannochloropsis gaditana*

**M. S. N. Atikah [1], W. A. K. G. Wan Azlina [1], Y. H. Taufiq-Yap [2,3], Omar Mahmoud [4], A. S. El-Shafay [5,6], R. A. Ilyas [7,8] and Razif Harun [1,*]**

1   Department of Chemical and Environmental Engineering, Faculty of Engineering, Universiti Putra Malaysia (UPM), Serdang 43400, Malaysia; sitinuratikah_asper7@yahoo.com (M.S.N.A.); wanazlina@upm.edu.my (W.A.K.G.W.A.)
2   Faculty of Science and Natural Resources, Universiti Malaysia Sabah, Kota Kinabalu 88400, Malaysia; taufiqyap@ums.edu.my
3   Catalysts Science and Technology Research Centre (PutraCAT), Faculty of Science, Universiti Putra Malaysia, Serdang 43400, Malaysia
4   Petroleum Engineering Department, Faculty of Engineering and Technology, Future University in Egypt, New Cairo 11835, Egypt; omar.saad@fue.edu.eg
5   Department of Mechanical Engineering, College of Engineering, Prince Sattam bin Abdulaziz University, Alkharj 16273, Saudi Arabia; a.abdou@psau.edu.sa
6   Mechanical Power Engineering Department, Faculty of Engineering, Mansoura University, Mansoura 35516, Egypt
7   School of Chemical and Energy Engineering, Faculty of Engineering, Universiti Teknologi Malaysia, Johor Bahru 81310, Malaysia; ahmadilyas@utm.my
8   Centre for Advanced Composite Materials, Universiti Teknologi Malaysia, Johor Bahru 81310, Malaysia
*   Correspondence: mh_razif@upm.edu.my; Tel.: +60-03-97696289

**Abstract:** A thermal behavior study of lipid-extracted *Nannochloropsis gaditana* (LEA) was performed in a thermogravimetric analyzer. The study was performed by heating the sample under different heating rates (5, 10, and 15 °C/min) from room temperature to 1000 °C using $N_2$ gas as the medium. This is crucial for thermal stability studies in a kinetic control regime. The following three stages of chemical decompositions were found: (1) moisture removal (2) devolatilization (3) fixed carbon decomposition; maximum decomposition was observed at the second stage. Activation energies of the LEA were studied using the Flynn–Wall–Ozawa model and Kissinger–Akahira–Sunose model. Main sample decomposition was observed from 100–700 °C during volatile matter evaporation. The thermal behavior study findings were used for the gasification of the sample with air to study the effect of varying reaction parameters on the compositions of the synthesis gas yield. Maximum $H_2$ yield was found at 700 °C and 0.7 g, which were 51.2 mol% and 50.6 mol%, respectively. From the study, it was found that LEA is suitable to be used as feedstock in gasification for synthesis gas production.

**Keywords:** lipid-extracted algae; thermogravimetric analysis; kinetics model; gasification; syngas

## 1. Introduction

Algae biofuel is known to be a good substitute for fossil fuels leading to the research and development of many aspects of the topic to investigate its viability and sustainability. Exploration of algae as a biofuel source is also associated with the limitation of lignocellulosic biomass as a second-generation biomass, e.g., with a complex structure as well as intensive and expensive pretreatments [1]. Algal biofuel is manufactured from microalgae biomass such as green algae species *Chorella* sp., *Dunaliella salina*, *Scenedesmus* sp., [2], and *Chamydomonas reinhardtii*, since they are capable of accumulating a high amount of lipids—up to 60%—within a short period of time due to their rapid reproduction rate [3]. They can be converted into renewable biofuel oil or gas which is more sustainable than fossil fuels [4]. Microalgae are unicellular photosynthetic simple plants that convert sunlight,

water, and carbon dioxide into chemical energy contained in the microalgal biomass [3,5]. *Nannochloropsis* sp. produces 20 tons of oil per hectare, which is 3.5 times greater than palm oil and 20 times that of sunflower and rapeseed [6]. Microalgae can fix $CO_2$ 10 to 50 times better than terrestrial plants [7], and they consume nutrients from runoff water from nearby land areas or by channeling sewage or wastewater treatment plants since they can be cultivated in fresh-, salt-, brackish-, and wastewater [4]. They can also be cultivated in open ponds or closed photobioreactors [8].

Algae biofuel is manufactured in the following three stages: (1) cultivation of microalgae, (2) biomass harvesting, and (3) manufacturing of the desired products [8,9]. Algal oil is extracted from the microalgal biomass after harvesting through physical, chemical, and biochemical approaches prior to transesterification of crude algal oil to crude biofuel. Microalgae also can be fermented for direct ethanol synthesis or undergo thermochemical conversion to produce synthesis gas (syngas) that are fuel gases [8,10]. *Nannochloropsis gaditana* lipid extracted algae (LEA) used in this study was obtained from the subcritical water extraction of algal oil under certain experimental conditions.

The thermochemical method of conversion of LEA offers simpler pathways from feedstock to product and is more advantageous than biochemical conversion [11]. Raheem et al. [12] reported that gasification is the most efficient method of conversion of biomass to gaseous products, since it is suitable for application with a wide range of biomasses, for instance, algae, palm oil waste, wood, peat, and solid waste. Thermogravimetric analysis (TGA) is used for biomass lignocellulosic composition determination, such as lignin, cellulose, and hemicelluloses [13,14], pyrolysis of biomass [15–18], combustion of palm oil biomass [19], reaction kinetics analysis [20], gasification of biomass [21,22], and torrefaction of wood [23]. They were performed by varying process parameters to mimic the actual process that aims to predict the behavior of the respective biomasses under certain thermal treatment processes. TGA is also performed for proximate analysis determination [21,24] since the thermogravimetric (TG) curve and first-order derivative of the thermogravimetric curve (DTG) is used to analyze the decomposition rate of the feedstock.

Different temperatures of the TGA process indicate different material losses. For instance, moisture (M) is released at 120 °C [13], below 150 °C [15,19], in the range of 100–150 °C [16], at 110 °C [17], and below 220 °C [14]. The difference in the temperature of moisture removal depends on the atmosphere, or the carrier gas used [21]. Volatile matter (VM) evaporation occurred at a temperature range from moisture removal, at up to 550 °C [13], up to 580 °C [15], 485–600 °C [25], up to 490 °C and 628 °C under $N_2$ and air atmosphere, respectively [21]. The next peak on the DTG curve above 500 °C denotes fixed carbon (FC) content, and the final composition of the feedstock indicates ash content in the feedstock.

In this study, the LEA was from subcritical water extraction (SWE) of algal oil. To the best of our knowledge, no studies are available in the literature reporting the thermal behavior of LEA from the subcritical water extraction (SWE) of algal oil. The TGA process of LEA was conducted using $N_2$ at different heating rates (5, 10, and 15 °C/min) from room temperature to 1000 °C, and the thermal behavior of the samples during TGA was studied.

## 2. Materials and Methods

### 2.1. Materials

The material used in this study was lipid-extracted algae (LEA) from *Nannochloropsis gaditana* obtained from the subcritical water extraction (SWE) of algal oil. The LEA was in a solid form and crushed in a mortar and pestle and sieved using a sieve mesh to achieve 90 microns size.

### 2.2. Proximate Analysis

Determination of moisture (M), volatile matter (VM), fixed carbon (FC), and ash was carried out in a thermogravimetric analyzer (TGAA/SDTA851, Mettler Toledo, OH, USA). A total of 20 mg of each algae residue sample was put in an alumina crucible and was

heated in a furnace continuously from room temperature to 1000 °C under different heating rates (5, 10, and 15 °C/min), using $N_2$ as the carrier gas at 50.00 mL/min.

### 2.3. Ultimate Analysis

The elementary compositions of LEA were performed in a CHNS analyzer (LECO True Spec CHNS628, USA). This analysis revealed the organic elements in LEA in wt% of carbon (C), hydrogen (H), and oxygen (O) as well as sulfur (S) and nitrogen (N). Dried samples of about 3 mg were put in the analyzer and the analysis was run at 1000 °C in the presence of oxygen, nitrogen, and helium as the carrier gases, and the elemental compositions were automatically calculated by the analyzer. The ultimate analysis data are useful in the computation of a higher heating value (HHV) by using Dulong's formula in Equation (1):

$$HHV = 0.3383 \times C + 1.443 \times (H\text{-}O/8) + 0.0942 \times S \tag{1}$$

where C, H, O, and S are mass fractions of carbon, hydrogen, oxygen, and sulfur in wt% of the samples [26]. This method is applicable for samples that are less than 1 g and are not enough for the bomb calorimetry test for calorific value.

### 2.4. Thermogravimetric Analysis (TGA)

A thermogravimetric analyzer (TGAA/SDTA851, Mettler Toledo, OH, USA) was used for thermal degradation. The gasification experiments were carried out by varying the heating rate from 5–25 °C/min with 5 °C/min increment using $N_2$ as a carrier gas under dynamic conditions with a flow rate of 50.00 mL/min. The gasification temperatures were raised from room temperature to 1000 °C. The duration of each experiment depends on the heating rate of TGA. The mass and heat transfer problem was overcome by fixing the mass of samples to 20 mg. After weighing the sample, it was directly placed into a 150 μL ceramic crucible and the temperature was kept isothermal for about one minute until a steady condition was obtained before increasing to 1000 °C. LEA weight loss and rate of weight loss were measured and recorded continuously as a function of temperature and time. Thermogravimetric (TG) and derivative thermogravimetric (DTG) curves of each sample were obtained as an output. These curves were used to analyze the thermal characteristics of LEA.

### 2.5. Gasification Experiments

LEA was gasified in a vertical fixed bed Temperature Programmed Gasifier (TPG) (model: VSTF50/150-1100, 1.2 kW/6 A) equipped with a type K thermocouple and connected to a digital gas flowmeter (model: FMA5506A; Omega Engineering, Inc., Selangor, Malaysia). There were two parameters studied at five levels, namely the reaction temperature (600, 700, 800, 900, and 1000 °C) and biomass loading (03, 0.4, 0.5, 0.6, and 0.7 g). ER, biomass loading, and airflow are correlated to each other in the ER formula, given in Equation (2):

$$ER = \frac{\frac{\text{mass of air}}{\text{mass of biomass}}}{\left(\frac{\text{mass of air}}{\text{mass of biomass}}\right)\text{stoichiometric}} \tag{2}$$

The gasifying medium used was compressed air, with a volumetric flow rate depending on the parameters being tested. Syngas from the reaction was passed through 8″ molecular sieves moisture trap, cotton wool, and ice bath to remove moisture and particles from the syngas. The syngas was then collected in a 3 L Tedlar gas storage bag and the inlet was sealed with plastic paraffin film (Parafilm) to minimize gas loss before further analysis of the syngas.

### 2.6. Syngas Analysis

The produced syngas was analyzed in a Gas Chromatograph with a Flame Ionization Detector (GC-FID). A Gas Chromatography with Flame Ionization Detector (GC-FID) (Agilent Technologies, 6890 N) was used in the syngas analysis to study the mole compositions

of desired gases, namely hydrogen ($H_2$), carbon monoxide (CO), carbon dioxide ($CO_2$), and methane ($CH_4$) in the syngas. Analysis of the syngas was carried out according to ASTM Method D3612-96. The sample gas was injected into a 30 m $\times$ 0.53 mm Carboxen-1010 PLOT column. The oven was set at 350 °C and argon gas was used as carrier gas under a 3.0 mL/min flow. The presence and composition of $H_2$, CO, $CO_2$, and $CH_4$ were analyzed from the chromatogram generated from GC-FID in parts per million (ppm) unit.

### 2.7. Kinetic Study of Gasification

TGA provides the measurement of weight loss as a function of temperature and time that is useful as a tool for comparing kinetic data of various reaction parameters [16]. Two iso-conversional models were used to calculate the activation energy of the gasification processes, namely the Kissinger–Akahira–Sunose (KAS) model and the Flynn–Wall–Ozawa (FWO) model. These kinetic models require TGA from any type of biomass, where TGA provides the data for weight loss as a function of temperature [16]. There were five different heating rates used (5, 10, and 15 °C/min).

The isoconversional method is based on the assumption that the conversion, $\alpha$ is expressed as a product of two functions that are independent of each other; k(T), which is solely dependent on the temperature, and f($\alpha$) which is dependent on the conversion of the decomposition process. In the non-isothermal decomposition of solid biomass, the sample mass was recorded as a function of temperature, where the general rate of thermal decomposition is expressed as:

$$\frac{d\alpha}{dt} = k(T)f(\alpha); \alpha = \frac{(w_o - w)}{(w_o - w_f)} \tag{3}$$

where $w_o$ is the initial weight of the sample, w is the weight of the sample at the corresponding time (min) or temperature (K), and the $w_f$ is the final weight of the sample after the reaction [27,28]. The rate of the reaction can be defined by the Arrhenius equation,

$$k = A \, e^{\left(-\frac{E}{RT}\right)} \tag{4}$$

where A ($min^{-1}$) is the pre-exponential factor of the Arrhenius equation, E ($J \, mol^{-1}$) is the activation energy, and R (8.314 $J \, mol^{-1} \, K^{-1}$) is the universal gas constant. Algae biomass is a multi-component mixture, hence, the complexity of the reaction increases with conversion ($\alpha$) [28]. This resulted in an extremely low possibility that different components have the same activation energy (Ea). Consequently, Ea and A are the functions of $\alpha$. At a constant heating rate of the sample ($\beta$ = dT/dt), the substitution of Equation (4) into Equation (3) resulted in Equation (5).

$$\frac{d\alpha}{dt} = A \exp\left(-\frac{E}{RT}\right)f(\alpha) \tag{5}$$

The natural log of Equation (5) is expressed as Equation (6):

$$\ln\left(\frac{d\alpha}{dt}\right) = \ln[A(\alpha)f(\alpha)] - \frac{E_a(\alpha)}{RT} \tag{6}$$

This equation is the basis for the Friedman method. Temperature is a function of time and increases with a constant heating rate, $\beta$, as shown in Equation (8):

$$\beta = \frac{dT}{dt} = \frac{dt}{d\alpha} \times \frac{d\alpha}{dt} \tag{7}$$

Rearranging Equation (7) gives:

$$\frac{d\alpha}{dt} = \beta \frac{d\alpha}{dT}; \frac{d\alpha}{dT} = \frac{1}{\beta} \frac{d\alpha}{dt} \tag{8}$$

Substituting Equation (8) into Equation (5) gives:

$$\frac{d\alpha}{dT} = \frac{1}{\beta} A e^{\left(-\frac{E_a}{RT}\right)} f(\alpha) \tag{9}$$

Equation (10) is the integrated form of Equation (9). Different kinetics methods were developed from this equation,

$$g(a) = \int_0^\alpha \frac{d\alpha}{f(\alpha)} = \int_0^T \frac{A}{\beta} e^{\left(-\frac{E}{RT}\right)} dT \tag{10}$$

where g(a) = integrated form of conversion dependence f($\alpha$), x = E/RT, A = constant, R = universal gas constant, 8.314 kJ mol K$^{-1}$, $\alpha$ = conversion value, and T = temperature in unit K. Different kinetic methods are applied in the study of thermal degradation of biomass from this equation [29,30].

The activation energy and pre-exponential factor were determined using two kinetics methods The first is (1) the Kissinger–Akahira–Sunose (KAS) method, adapted from Kissinger, 1957,

$$\ln\left(\frac{\beta}{T^2}\right) = \ln\left(\frac{AE}{Rg(a)}\right) - \left(\frac{E}{RT}\right) \tag{11}$$

and the second is the (2) Flynn–Wall–Ozawa (FWO) method, adapted from Flynn and Wall., 1966,

$$\ln \beta = \ln\left[\frac{AE}{Rg(\alpha)}\right] - 5.331 - 1.052\frac{E}{RT} \tag{12}$$

The activation energy for the specified value of conversion, $\alpha$, of the thermal decomposition reaction is obtained from the slope of the curves, $ln\left(\frac{\beta}{T^2}\right)$ versus $\frac{1}{T}$ ($-1.052E/R$) and $\ln\beta$ versus $1/T$ ($-E/R$) for the KAS and FWO models, respectively [21,30,31]. Repeating the activation energy determination for the whole range of $\alpha$ from 0 to 1 will result in activation energy of progressing values of $\alpha$ for both models.

## 3. Results

### 3.1. Proximate Analysis

Proximate analysis data such as moisture, volatile matter, fixed carbon, and ash at different heating rates are as tabulated in Table 1. Figure 1 shows proximate analysis based on LEA on thermogravimetric (TG) and derivative thermogravimetric (DTG) curves at 15 °C/min heating rate. Table 2 shows the ultimate analysis data for LEA.

**Table 1.** Proximate analysis data for LEA from this study and other algal species from literature.

| | **This Study** | | | **Literature** | |
| | **LEA** | | | *Chorella* **sp. LEA [31]** | *T. suecica* **LEA [31]** |
|---|---|---|---|---|---|
| HR | 5 | 10 | 15 | 10 | 10 |
| M | 4.2 $\pm$ 0.5 | 5.2 $\pm$ 0.5 | 4.1 $\pm$ 0.6 | 6.0 | 6.0 |
| VM | 65.7 $\pm$ 0.9 | 63.4 $\pm$ 1.4 | 68.1 $\pm$ 2.2 | 56.0 | 54.0 |
| FC | 7.7 $\pm$ 1.4 | 5.9 $\pm$ 1.0 | 12 $\pm$ 0.7 | 18.0 | 20.0 |
| A | 23.1 $\pm$ 0.3 | 20.4 $\pm$ 0.2 | 9.3 $\pm$ 0.3 | 20.0 | 20.0 |

HR = heating rate (°C/min), M = moisture, VM = volatile matter, FC = fixed carbon, A = ash.
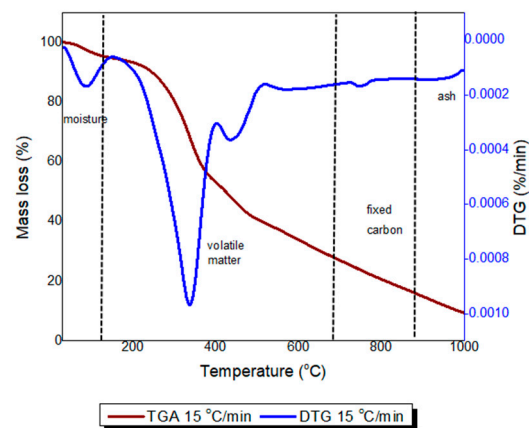
**Figure 1.** Proximate analysis based on LEA on TG and DTG curves at 15 °C/min heating rate.

**Table 2.** Ultimate analysis data for LEA.

| | This Study | | Literature | | |
|---|---|---|---|---|---|
| **wt%** | **LEA** | **LEA [32]** | ***Chorella* sp. LEA [31]** | ***T. suecica* LEA [31]** | ***Nannochloropsis* sp. LEA [33]** |
| C | 48.04 ± 0.1 | 47.91 | 39.34 | 24.09 | 50.6 |
| H | 7.27 ± 0.2 | 6.83 | 6.60 | 3.64 | 6.8 |
| N | 6.57 ± 0.1 | 7.56 | 7.91 | 4.12 | 5.6 |
| S | 0.64 ± 0.2 | 0.63 | 0.65 | 0.61 | 0.9 |
| O * | 37.48 ± 0.3 | 37.07 | 45.50 | 67.54 | 27.8 |
| HHV [a] (MJ kg$^{-1}$) | 20.60 | - | - | - | - |

* by difference, HHV [a] = high heating value.

The TGA was performed at 5, 10, and 15 °C/min heating rate under 50 mL/min nitrogen gas flow from 30 °C to 1000 °C. The TG and DTG curves for LEA are as shown in Figure 2. The mass loss percentage is represented by the TG curve, where the steeper region indicated greater mass loss. The DTG curve illustrated the rate of decomposition of the samples in %/min unit, where each peak in the DTG curve represents the decomposition of the samples that occurred in the following three stages: (1) moisture removal (2) devolatilization of volatiles (3) fixed carbon decomposition, that left the samples with only ash at the end of the analysis.
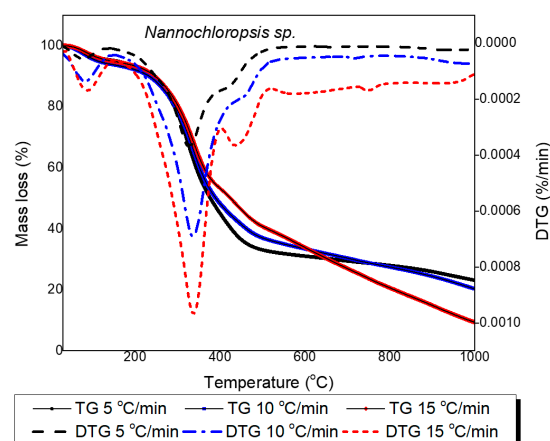


**Figure 2.** TG and DTG curves at 5, 10, and 15 °C/min.

Generally, algae are composed of lipids, carbohydrates, and proteins while lignocellulosic biomass contains, cellulose, hemicellulose, and lignin. Hence, some of the peaks found in DTG curves represent the decomposition of these components. The first peak at all heating rates indicated moisture removal, in which mass loss was associated with moisture in the samples that were eliminated. This stage occurred at 30–100 °C, where the highest peak was observed at 88.17 °C. This is in agreement with *Nannochloropsis* sp. LEA TGA in a study conducted by Marcilla et al. [34] showed that less than 10% of the overall mass decrement was obtained, which specified that less than 10% moisture was present in the samples before the analysis. The dehydrated samples then proceeded to decompose at higher temperatures, eliminating other chemical compounds in them.

The reaction was then processed at a high rate, as observed at the second peak, where devolatilization of volatiles in the samples occurred at 100–700 °C. This stage can be further divided into two regions, where the first region is in the temperature range of 100–400 °C and the second region is in the range of 400–700 °C. This is due to the presence of more than one peak along the stage that was caused by the decomposition of different chemical compounds. Sanchez-Silva et al. [35] reported that the decomposition of carbohydrates and protein takes place at 180–450 °C. This temperature range is similar to the decomposition of cellulose, hemicellulose, and lignin in woody biomass, at 200–430 °C, 250–350 °C, and 250–550 °C, respectively. In this study, $T_{max}$ for gasification in the first region of the second stage was obtained at 338.15 °C, which is an indication that lower heat energy is required for the decomposition of algal biomass compared to woody and lignocellulosic biomasses. A few peaks were observed at the second region of volatile matter release at 400–700 °C. This region is associated with the decomposition of remaining proteins and other inorganic compounds that proceeded at a slower rate [36]. At this stage, pyrolysis products such as combustible gases, tar, and char are produced [21].

Lower weight loss was found at the third peak, at 700–900 °C due to the fixed carbon being surrounded by ash after the devolatilization of volatile matter. Beyond 600 °C, the fixed carbon combustion was close to the terminal, and a DTG peak formed when the combustion reached the terminal [37]. This peak was observed at 750.8 °C. A summary of all the stages during gasification is illustrated in Table 3.

**Table 3.** Kinetics data for sample decomposition at different stages.

| | Stage | | | | | | | | | | | | Final Ash at 1000 °C (%) |
|---|---|---|---|---|---|---|---|---|---|---|---|---|---|
| | **I** | | | **II** | | | | | | **III** | | | |
| **HR** | | | | **Region 1** | | | **Region 2** | | | | | | |
| | **ML (%)** | **AR (%/min)** | **$T_{max}$ (°C)** | **ML (%)** | **AR (%/min)** | **$T_{max}$ (°C)** | **ML (%)** | **AR (%/min)** | **$T_{max}$ (°C)** | **ML (%)** | **AR (%/min)** | **$T_{max}$ (°C)** | |
| 5 | 4.18 | 0.23 | 99.6 | 43.07 | 0.77 | 343.0 | 23.32 | 0.39 | 401.0 | 6.35 | 0.16 | 702.3 | 23.08 |
| 10 | 5.28 | 0.59 | 77.7 | 46.60 | 1.67 | 343.5 | 17.76 | 0.59 | 405.0 | 10.01 | 0.50 | 715.5 | 20.35 |
| 15 | 4.12 | 0.69 | 96.8 | 50.75 | 2.73 | 343.3 | 21.32 | 1.07 | 401.5 | 14.47 | 1.09 | 743.0 | 9.34 |

HR = heating rate (°C/min), ML = mass loss, AR = average reaction rate, $T_{max}$ = temperature of maximum degradation determined from DTG peaks.

### 3.2. Effect of Heating Rate on Samples Decomposition

The TGA analysis was performed at different heating rates of 5, 10, and 15 °C/min. Table 3 showed that the heating rate influenced mass loss, the maximum temperature of degradation, and final ash content at the end of the analysis. The increase in the heating rate decreased the formation of residue or ash at the end of the analysis at 1000 °C. This trend is in good agreement with findings from another study conducted by Asyraf et al. [31] for the pyrolysis of *Chorella* sp. and Tetraselmis suecica LEA. The study proved that a higher heating rate is associated with a higher rate of devolatilization of volatiles from the biomass which also explains the lower ash content at higher heating rates. In addition, thermal

equilibrium within the biomass particles took a longer time to be achieved resulting in the maximum temperature of degradation shifting towards higher temperatures.

### 3.3. Kinetic Study of Gasification

Gasification of LEA was carried out at 30–1000 °C under an $N_2$ atmosphere at three different heating rates (5, 10, 15 °C/min). The increment in heating rates increased the decomposition percentage, as illustrated in Table 3 which resulted in a lower ash content at the end of the analysis. This is due to the higher rate of volatiles released at higher heating rates, as seen for mass loss for the volatile matter at stage II for all heating rates and samples with increasing trend.

Increasing heating rates also resulted in $T_{max}$ of all stages shifting towards higher temperatures, as observed in a study by Asyraf et al. [31] for the decomposition of *Chorella* sp. and *Tetraselmis suecica* LEA. The result is also consistent with work of Shuping et al. [29] for pyrolysis of *Dunaliella tertiolecta* biomass at heating rates of 5, 10, 20, and 40 °C/min. Kongkaew et al. [38] also reported the same findings for the pyrolysis of rice straw. This was due to the nature of the biomasses themselves, which are poor heat conductors, thus producing a temperature gradient throughout their particles. This also could be explained by the limitation of heat transfer. At lower heating rates, a longer time is required to produce equilibrium in temperature at the outer face and inner core of the particles. At the same time and in temperature regions at higher heating rates, the reaction rate was shortened, thus the biomass particles' cores possessed lower temperatures than at their outer surface. A higher temperature is required for the biomass core and outer surface to reach equilibrium and the devolatilization rates of the biomass to differ at different heating rates [31,38].

### 3.4. Activation Energy (E)

The analysis of activation energy (E) was performed using KAS and FWO models. For the FWO model, the plot of ln β against 1/T produced straight lines at the different conversions of the biomass samples. For the KAS model, the plot of ln $(\beta/T^2)$ against 1/T also generated straight lines at different conversion α values, as illustrated in Figure 3a,b. E values were obtained from the slopes of these plots with high $R^2$ values > 0.75, thus proving that the data are valid in the values of E determination. The activation energy values were determined from the slope of the straight line plots, where α values were the decomposition of the samples that ranged from 0 to 1.
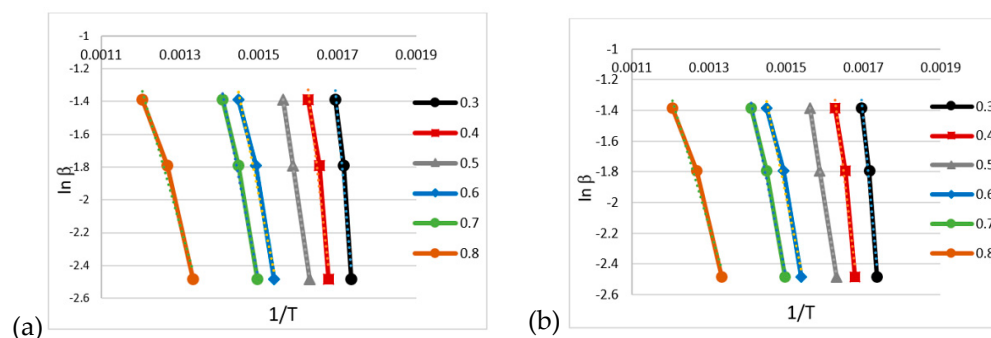


**Figure 3.** Plots for activation energy for determination for LEA (**a**) FWO model (**b**) KAS model.

The best prediction of activation energy was at 0.3 < α < 0.8. α; values below 0.3 predicted the activation energy for moisture removal instead of thermal decomposition of the algae residues and α values beyond 0.8 were associated with ash formation [39]. In addition, the range of α values selected is wide enough for volatile matter devolatilization and fixed carbon decomposition for LEA, indicated by the temperature range at 0.3 < α < 0.8.

Table 3 shows the results of proximate analysis from LEA which consist of the percentage of mass loss (ML) and average decomposition rate (AR). Stage II was where the

devolatilization process occurred, where most of the volatiles in the biomass were released. The pattern of mass loss was increased at region 1 which occurred in the temperature range of 121–400 °C. This was ascribed to the decomposition of the soluble proteins and polysaccharides present in LEA [31]. The second region of stage II occurred from 401–700 °C, whereby the degradation of insoluble polysaccharides and crude lipids took place. The trend of the mass loss is inconsistent with the variation in heating rate. For all stages of thermal decomposition, the trend of average decomposition rate, and AR were found to increase with the heating rate which resulted in a decreasing percentage of ash left at the end of the process.

Table 4 summarizes the activation energy obtained from both models at different conversion values. It was found that all plots have high correlation coefficients ($R^2$) values, as shown in the table. For both the KAS and FWO models, the activation energy values varied with $\alpha$ and heating rate, in which the decomposition of different compounds took place at different $\alpha$ values for different heating rates. As the heating rates increased, the temperatures at all respective $\alpha$ values decreased, as observed in Table 4. This phenomenon is associated with a higher percentage of mass loss, ML, as the heating rates increased, as observed in Table 3 [31]. The highest activation energy values were obtained at $\alpha = 0.3$ which fell in the first region of stage II decomposition. This is supported by the AR from Table 3 that were found to be the highest in this region of 2.73%/min.

**Table 4.** Activation energy obtained from KAS and FWO models for both samples' gasification.

| Decomposition ($\alpha$) | Temperature (°C) | KAS | | FWO | |
|---|---|---|---|---|---|
| | | E (kJ mol$^{-1}$) | $R^2$ | E (kJ mol$^{-1}$) | $R^2$ |
| 0.3 | 323, 310, 303 | 215.59 | 0.9696 | 214.15 | 0.9721 |
| 0.4 | 347, 332, 323 | 167.09 | 0.9600 | 168.41 | 0.9644 |
| 0.5 | 386, 351, 341 | 125.75 | 0.9777 | 129.42 | 0.9999 |
| 0.6 | 452, 379, 363 | 91.52 | 0.9999 | 97.58 | 0.9825 |
| 0.7 | 559, 427, 395 | 92.78 | 0.9851 | 99.08 | 0.9883 |
| 0.8 | 689, 515, 436 | 57.99 | 0.9667 | 67.58 | 0.9784 |

Temperature = temperature at different heating rates (5, 10 and 15 °C/min) with respect to $\alpha$ values, SR = seaweeds residue.

### 3.5. Gasification of LEA

Gasification is a high-temperature conversion of feedstock in which the solid is converted into gaseous mixtures such as $H_2$, CO, $CO_2$, $CH_4$, light hydrocarbons, tar, char, ash, and minor contaminates at atmospheric pressure in an environment of insufficient oxidizer [40,41]. In this study, the gasification experiments were carried out in a temperature programmed gasifier (TPG) and the collected gas was tested in a GC-FID. The results of the gasification experiments are as stated in Table 5.

### 3.5.1. Effect of Temperature

The gasification temperatures used in this study were in a range of (600–1000 °C) with a 100 °C increment. The biomass loading and ER were kept constant at 0.4 g and 0.25, respectively. LEA gasification is an endothermic process that requires a supply of heat to shift the gasification reactions to the right. All endothermic processes that occurred during gasification were favored as the temperature increased. It was found that the $H_2$ increased as the temperature increased as shown in Table 5. The highest $H_2$ composition was 51.2 mol% at 700 °C; meanwhile, CO yield was highest at 1000 °C, which was 54.4 mol% for LEA from the experiment. Slightly different values of 51.85 mol% $H_2$ and 48.01 mol% CO were obtained with the simulated results. However, $H_2$ yields were decreased to 48.5 mol% and 50.38 mol% at 800 °C for the experimental and predicted $H_2$ yields, respectively.

**Table 5.** Effect of temperature and loading in gasification for LEA and seaweeds. Results presented are average values from 2 replicates.

| | Experimental Parameters | | | Syngas Composition (mol%) | | | |
|---|---|---|---|---|---|---|---|
| | Temp (ºC) | Loading (g) | ER | $H_2$ | CO | $CO_2$ | $CH_4$ |
| Effect of temperature | 600 | 0.4 | 0.25 | 47.8 ± 0.2 | 20.1 ± 0.9 | 25.9 ± 0.1 | 7.0 ± 0.8 |
| | 700 | 0.4 | 0.25 | 51.2 ± 0.8 | 33.3 ± 0.7 | 11.2 ± 0.6 | 5.3 ± 0.5 |
| | 800 | 0.4 | 0.25 | 48.5 ± 0.5 | 46.2 ± 0.8 | 3.9 ± 0.2 | 3.4 ± 0.6 |
| | 900 | 0.4 | 0.25 | 45.6 ± 0.4 | 49.6 ± 0.4 | 2.6 ± 0.3 | 2.1 ± 0.7 |
| | 1000 | 0.4 | 0.25 | 40.7 ± 0.3 | 54.4 ± 0.6 | 2.3 ± 0.7 | 1.9 ± 0.4 |
| Effect of loading | 700 | 0.3 | 0.25 | 28.3 ± 0.7 | 16.4 ± 0.6 | 22.6 ± 0.4 | 31.3 ± 0.7 |
| | 700 | 0.4 | 0.25 | 33.1 ± 0.9 | 14.3 ± 0.7 | 20.3 ± 0.7 | 30.2 ± 0.8 |
| | 700 | 0.5 | 0.25 | 45.6 ± 0.4 | 5.0 ± 0.8 | 18.3 ± 0.7 | 33.5 ± 0.5 |
| | 700 | 0.6 | 0.25 | 47.0 ± 1.2 | 4.6 ± 0.4 | 16.6 ± 0.6 | 33.9 ± 0.1 |
| | 700 | 0.7 | 0.25 | 50.6 ± 0.4 | 2.9 ± 0.3 | 10.9 ± 0.5 | 37.6 ± 0.7 |

This can be explained by the minimal impact of the water–gas–shift reaction ($CO + H_2O \leftrightarrow H_2 + CO_2$) that resulted in the consumption of both $H_2$ and $CO_2$ and boosted the production of CO [42]. In addition, the major gases obtained were $H_2$ and CO, which indicated that the major reactions involved in the gasification were oxidation, water–gas, and water–gas–shift reactions [35]. A Bouduard reaction, which is an endothermic reaction, also contributed to the increase in CO compositions due to the $CO_2$ reaction with char to produce CO [43]. This resulted in an increment of CO with temperature.

### 3.5.2. Effect of Loading

The effect of loading was investigated by manipulating biomass loading (0.3, 0.4, 0.5, 0.6, and 0.7 g) while temperature and ER were kept constant at 700 °C and 0.25, respectively. Table 5 shows that the $H_2$ yield increased from 28.3 mol% to 50.6 mol% as the loading increased from 0.3 g to 0.7 g due to the occurrence of water–gas shift reaction, methanation reaction, and dry reforming reaction [21,43]. Raheem et al. [12] reported that the increasing ratio of biomass improved the yield of $H_2$ and $CH_4$ in the syngas, as well as the total carbon conversion and gasification efficiency. CO yield decreased as the loading increased, which was from 16.4 mol% to 2.9 mol%. This is due to the enhancement of the water–gas shift reaction at higher loading that promoted $H_2$ and suppressed CO production.

### 4. Conclusions

Thermogravimetric analysis of *Nannochloropsis gaditana* LEA was carried out in a thermogravimetric analyzer (TGA) at 30–1000 °C under $N_2$ flow as the carrier gas. As observed from the analysis, the following three stages of decomposition occurred: moisture release as observed at the first peak of DTG curves, pyrolysis of organic materials at the second peak, solid residue decomposition, or fixed carbon release at the third peak. From these stages, maximum degradations were observed at the second stage at all heating rates. An increase in the heating rate increased the devolatilization of volatiles rate, which resulted in a lower ash content as well as maximum degradation temperature that was also ascribed by thermal equilibrium within the samples' particles. The highest activation energy was found at $\alpha = 0.3$, which fell under the devolatilization stage, proven by the highest AR value found at this stage. Gasification of LEA also was carried out at two different parameter variables, where the highest $H_2$ yield was attained at 800 °C and 0.7 g. Since gasification of LEA showed a considerably high $H_2$ yield and requires low activation energy, LEA was found to be suitable to be used in gasification for syngas production.

In the future, a kinetics analysis of other species of LEA could be performed to study the suitability of samples for gasification. This could, in turn, maximize the utilization of microalgae for producing value-added products.

**Author Contributions:** Conceptualization, M.S.N.A. and R.H.; methodology, M.S.N.A. and R.H.; validation, W.A.K.G.W.A. and Y.H.T.-Y.; formal analysis, M.S.N.A. and R.H.; investigation, M.S.N.A. and R.H.; resources, M.S.N.A. and R.H.; data curation, M.S.N.A. and R.H.; writing—original draft preparation, M.S.N.A. and R.H.; writing—review and editing, M.S.N.A., W.A.K.G.W.A., R.H., Y.H.T.-Y., O.M., A.S.E.-S. and R.A.I.; visualization, O.M., A.S.E.-S. and R.A.I.; supervision, W.A.K.G.W.A., R.H. and Y.H.T.-Y.; funding acquisition, O.M. All authors have read and agreed to the published version of the manuscript.

**Data Availability Statement:** Not applicable.

**Conflicts of Interest:** The authors declare no conflict of interest.

## Abbreviations

| | |
|---|---|
| **LEA** | Lipid-extracted algae |
| **TGA** | Thermogravimetric analysis/Thermogravimetric analyzer |
| **H$_2$** | Hydrogen |
| **CO** | Carbon monoxide |
| **CH$_4$** | Methane |
| **CO$_2$** | Carbon dioxide |
| **ER** | Equivalence ratio |
| **GC-FID** | Gas Chromatography with Flame Ionization Detector |
| **SWE** | Subcritical water extraction |
| **KAS** | Kissinger-Akahira-Sunose |
| **FWO** | Flynn-Wall-Ozawa |
| **HHV** | High heating value |
| **TPG** | Temperature Programmed Gasifier |

## References

1. Khoo, C.G.; Dasan, Y.K.; Lam, M.K.; Lee, K.T. Algae Biorefinery: Review on a Broad Spectrum of Downstream Processes and Products. *Bioresour. Technol.* **2019**, *292*, 121964. [CrossRef] [PubMed]
2. Yang, Z.; Guo, R.; Xu, X.; Fan, X.; Luo, S. Hydrogen and Methane Production from Lipid-Extracted Microalgal Biomass Residues. *Int. J. Hydrogen Energy* **2011**, *36*, 3465–3470. [CrossRef]
3. Scott, S.A.; Davey, M.P.; Dennis, J.S.; Horst, I.; Howe, C.J.; Lea-Smith, D.J.; Smith, A.G. Biodiesel from Algae: Challenges and Prospects. *Curr. Opin. Biotechnol.* **2010**, *21*, 277–286. [CrossRef] [PubMed]
4. Demirbas, A. Use of Algae as Biofuel Sources. *Energy Convers. Manag.* **2010**, *51*, 2738–2749. [CrossRef]
5. Ansari, F.A.; Nasr, M.; Guldhe, A.; Gupta, S.K.; Rawat, I.; Bux, F. Techno-economic feasibility of algal aquaculture via fish and biodiesel production pathways: A commercial-scale application. *Sci. Total Environ.* **2019**, *704*, 135259. [CrossRef] [PubMed]
6. Padovani, G.; Rodolfi, L.; Zittelli, G.C.; Biondi, N.; Bonini, G.; Tredici, M.R.; Agrarie, B. Microalgae for Oil: Strain Selection, Induction of Lipid Synthesis and Outdoor Mass Cultivation in a low-cost photobioreactor. *Biotechnol. Bioeng.* **2009**, *102*, 100–112. [CrossRef]
7. Raheem, A.; Wan Azlina, W.A.K.G.; Tau, Y.H.; Danquah, M.K. Thermochemical Conversion of Microalgal Biomass for Biofuel Production. *Renew. Sustain. Energy Rev.* **2015**, *49*, 990–999. [CrossRef]
8. NRC. *Sustainable Development of Algal Biofuels in the United States*; National Academies Press: Washington, DC, USA, 2012; Volume 7, ISBN 9780309260329.
9. Said, Z.; Trong, D.; Le, N.; Sharma, P.; Ha, V.; Son, H.; Tuyen, D.; Anh, T.; Bui, E.; Nguyen, V.G. Optimization of Combustion, Performance, and Emission Characteristics of a Dual-Fuel Diesel Engine Powered with Microalgae-Based Biodiesel/Diesel Blends and Oxyhydrogen. *Fuel* **2022**, *326*, 124987. [CrossRef]

10. Sharma, P.; Sahoo, B.B. An ANFIS-RSM Based Modeling and Multi-Objective Optimization of Syngas Powered Dual-Fuel Engine. *Int. J. Hydrogen Energy* **2022**, *47*, 19298–19318. [CrossRef]

11. Sims, R.E.H.; Mabee, W.; Saddler, J.N.; Taylor, M. An Overview of Second Generation Biofuel Technologies. *Bioresour. Technol.* **2010**, *101*, 1570–1580. [CrossRef]

12. Raheem, A.; Wan Azlina, W.A.K.G.; Yap, Y.H.T.; Danquah, M.K.; Harun, R. Optimization of the Microalgae Chlorella Vulgaris for Syngas Production Using Central Composite Design. *RSC Adv.* **2015**, *5*, 71805–71815. [CrossRef]

13. Carrier, M.; Loppinet-serani, A.; Denux, D.; Lasnier, J. Thermogravimetric Analysis as a New Method to Determine the Lignocellulosic Composition of Biomass. *Biomass Bioenergy* **2010**, *35*, 298–307. [CrossRef]

14. Serapiglia, M.J.; Cameron, K.D.; Stipanovic, A.J.; Smart, L.B. Analysis of Biomass Composition Using High-Resolution Thermogravimetric Analysis and Percent Bark Content for the Selection of Shrub Willow Bioenergy Crop Varieties. *Bioenergy Resour.* **2009**, *2*, 1–9. [CrossRef]

15. Shawalliah, S.; Abd, N.; Ismail, K.; Bahari, A.; Abd, Z. Investigation on Thermochemical Behaviour of Low Rank Malaysian Coal, Oil Palm Biomass and Their Blends during Pyrolysis via Thermogravimetric Analysis (TGA). *Bioresour. Technol.* **2010**, *101*, 4584–4592. [CrossRef]

16. Vuthaluru, H.B. Investigations into the Pyrolytic Behaviour of Coal/Biomass Blends Using Thermogravimetric Analysis. *Bioresour. Technol.* **2004**, *92*, 187–195. [CrossRef]

17. Stenseng, M.; Jensen, A.; Dam-johansen, K. Investigation of Biomass Pyrolysis by Thermogravimetric Analysis and Differential Scanning Calorimetry. *J. Anal. Appl. Pyrolysis* **2001**, *59*, 765–780. [CrossRef]

18. Chang, Y.M.; Tsai, W.T.; Li, M.H. Chemical Characterization of Char Derived from Slow Pyrolysis of Microalgal Residue. *J. Anal. Appl. Pyrolysis* **2015**, *111*, 88–93. [CrossRef]

19. Shawalliah, S.; Abd, N.; Ismail, K. Combustion Characteristics of Malaysian Oil Palm Biomass, Sub-Bituminous Coal and Their Respective Blends via Thermogravimetric Analysis (TGA). *Bioresour. Technol.* **2012**, *123*, 581–591. [CrossRef]

20. Me, E.; Jakab, E. Thermogravimetric and Reaction Kinetic Analysis of Biomass Samples from an Energy Plantation. *Energy Fuels* **2004**, *18*, 497–507.

21. Raheem, A.; Sivasangar, S.; Wan Azlina, W.A.K.G.; Taufiq Yap, Y.H.; Danquah, M.K.; Harun, R. Thermogravimetric Study of Chlorella Vulgaris for Syngas Production. *Algal Res.* **2015**, *12*, 52–59. [CrossRef]

22. Chang, Y.M.; Tsai, W.T.; Li, M.H.; Chang, S.H. Preparation and Characterization of Porous Carbon Material from Post-Extracted Algal Residue by a Thermogravimetric System. *Algal Res.* **2015**, *9*, 8–13. [CrossRef]

23. Prins, M.J. Thermodynamic Analysis of Biomass Gasification and Torrefaction. Ph.D. Thesis, Eindhoven University of Technology, Eindhoven, The Netherlands, 2005.

24. Chang, Y.M.; Tsai, W.T.; Li, M.H. Characterization of Activated Carbon Prepared from Chlorella-Based Algal Residue. *Bioresour. Technol.* **2014**, *184*, 344–348. [CrossRef]

25. Varol, M.; Atimtay, A.T.; Bay, B.; Olgun, H. Investigation of Co-Combustion Characteristics of Low Quality Lignite Coals and Biomass with Thermogravimetric Analysis. *Thermochim. Acta* **2010**, *510*, 195–201. [CrossRef]

26. Biller, P. Hydrothermal Processing of Microalgae. Ph.D. Thesis, The University of Leeds, Leeds, UK, 2013.

27. Tahmasebi, A.; Asyraf, M.; Yu, J.; Bhattacharya, S. Thermogravimetric Study of the Combustion of Tetraselmis Suecica Microalgae and Its Blend with a Victorian Brown Coal in $O_2/N_2$ and $O_2/CO_2$ Atmospheres. *Bioresour. Technol.* **2013**, *150*, 15–27. [CrossRef]

28. Raheem, A.; Dupont, V.; Channa, A.Q.; Zhao, X.; Vuppaladadiyam, A.K.; Taufiq-Yap, Y.H.; Zhao, M.; Harun, R. Parametric Characterization of Air Gasification of Chlorella Vulgaris Biomass. *Energy Fuels* **2017**, *31*, 2959–2969. [CrossRef]

29. Shuping, Z.; Yulong, W.; Mingde, Y.; Chun, L.; Junmao, T. Pyrolysis Characteristics and Kinetics of the Marine Microalgae Dunaliella Tertiolecta Using Thermogravimetric Analyzer. *Bioresour. Technol.* **2010**, *101*, 359–365. [CrossRef]

30. Damartzis, T.; Vamvuka, D.; Sfakiotakis, S.; Zabaniotou, A. Thermal Degradation Studies and Kinetic Modeling of Cardoon (*Cynara cardunculus*) Pyrolysis Using Thermogravimetric Analysis (TGA). *Bioresour. Technol.* **2011**, *102*, 6230–6238. [CrossRef]

31. Kassim, M.A.; Kirtania, K.; De La Cruz, D.; Cura, N.; Srivatsa, S.C.; Bhattacharya, S. Thermogravimetric Analysis and Kinetic Characterization of Lipid-Extracted *Tetraselmis Suecica* and *Chlorella* sp. *ALGAL* **2014**, *6*, 39–45. [CrossRef]

32. Ho, B.C.H.; Harun, R. Extraction of Bioactive Compounds from Nannochloropsis Gaditana via Sub-Critical Water Extraction (SWE). *BioMed Res. Int.* **2016**, *14*, 19–24.

33. Tiong, L.; Komiyama, M. Statistical Analysis of Microalgae Supercritical Water Gasification: Reaction Variables, Catalysis and Reaction Pathways. *J. Supercrit. Fluids* **2022**, *183*, 105552. [CrossRef]

34. Marcilla, A.; Gómez-Siurana, A.; Gomis, C.; Chápuli, E.; Carmen, M.; Valdés, F.J. Characterization of Microalgal Species through TGA/FTIR Analysis: Application to *Nannochloropsis* sp. *Thermochim. Acta* **2009**, *484*, 41–47. [CrossRef]

35. Sanchez-Silva, L.; López-González, D.; Garcia-Minguillan, A.; Valverde, J. Pyrolysis, Combustion and Gasification Characteristics of Nannochloropsis Gaditana Microalgae. *Bioresour. Technol.* **2013**, *130*, 321–331. [CrossRef] [PubMed]

36. Kim, S.; Vu, H.; Kim, J.; Hyung, J.; Chul, H. Thermogravimetric Characteristics and Pyrolysis Kinetics of *Alga sagarssum* sp. Biomass. *Bioresour. Technol.* **2013**, *139*, 242–248. [CrossRef] [PubMed]

37. Yu, L.J.; Wang, S.; Jiang, X.M.; Wang, N.; Zhang, C.Q. Thermal Analysis Studies on Combustion Caracteristics of Seaweed. *J. Therm. Anal. Calorim.* **2008**, *93*, 611–617. [CrossRef]

38. Kongkaew, N.; Pruksakit, W.; Patumsawad, S. *Thermogravimetric Kinetic Analysis of the Pyrolysis of Rice Straw*; Elsevier B.V.: Amsterdam, The Netherlands, 2015; Volume 79.

39. Carpio, R.B.; Zhang, Y.; Kuo, C.; Chen, W.; Charles, L.; Leon, R.L. De Characterization and Thermal Decomposition of Demineralized Wastewater Algae Biomass. *Algal Res.* **2019**, *38*, 101399. [CrossRef]

40. Mikulandrić, R.; Lončar, D.; Böhning, D.; Böhme, R. Biomass Gasification Process Modelling Approaches. In Proceedings of the 8th Conference on Sustainable Development of Energy, Water and Environment Systems—SDEWES Conference, Dubrovnik, Croatia, 22–27 September 2013; pp. 1–13.

41. Chen, W.H.; Lin, B.J.; Huang, M.Y.; Chang, J.S. Thermochemical Conversion of Microalgal Biomass into Biofuels: A Review. *Bioresour. Technol.* **2014**, *184*, 314–327. [CrossRef]

42. Chen, W.; Hsieh, T.; Leo, T. An Experimental Study on Carbon Monoxide Conversion and Hydrogen Generation from Water Gas Shift Reaction. *Energy Convers. Manag.* **2008**, *49*, 2801–2808. [CrossRef]

43. Doherty, W.; Reynolds, A.; Kennedy, D. The Effect of Air Preheating in a Biomass CFB Gasifier Using ASPEN Plus Simulation. *Biomass Bioenergy* **2009**, *33*, 1158–1167. [CrossRef]